RESEARCH PAPER

Study of fractional order SIR model with M-H type treatment rate and its stability analysis

Subrata Paul [1,‡], **Animesh Mahata** [2,*,‡], **Supriya Mukherjee** [3,‡], **Meghadri Das** [4,‡], **Prakash Chandra Mali** [5,‡], **Banamali Roy** [6,‡], **Poulami Mukherjee** [7,‡] and **Pramodh Bharati** [8,9,‡]

[1]Department of Mathematics, Arambagh Govt. Polytechnic, Arambagh-712602, West Bengal, India, [2]Department of Mathematics, Sri Ramkrishna Sarada Vidya Mahapitha, Kamarpukur, Hooghly-712612, India, [3]Department of Mathematics, Gurudas College, 1/1 Suren Sarkar Road, Kolkata-700054, West Bengal, India, [4]Indian Institute of Engineering Science and Technology, Shibpur, Howrah-711103, West Bengal, India, [5]Department of Mathematics, Jadavpur University, 188 Raja S.C. Mallik Road, Kolkata-700032, West Bengal, India, [6]Department of Mathematics, Bangabasi Evening College, Kolkata-700009, West Bengal, India, [7]Department of Mathematics, Calcutta Girls' B.T. College, Ballygunge, Kolkata-700019, West Bengal, India, [8]Department of Mathematics, Ramnagar College, Purba Medinipur-721453, West Bengal, India, [9]Department of Mathematics, Swami Vivekananda University, Telinipara, Barasat-Barrackpore Rd, Bara Kanthalia, West Bengal-700121, India

* Corresponding Author
‡ paulsubrata564@gmail.com (Subrata Paul); animeshmahata8@gmail.com (Animesh Mahata); supriyaskbu2013@gmail.com (Supriya Mukherjee); dasmeghadri@gmail.com (Meghadri Das); pcmali1959@gmail.com (Prakash Chandra Mali); banamaliroy@yahoo.co.in (Banamali Roy); poulamimukherjee2023@gmail.com (Poulami Mukherjee); pramodbharatinilu@gmail.com (Pramodh Bharati)

Abstract

In this manuscript, we analyze a fractional-order susceptible-infected-recovered (SIR) mathematical model with a nonlinear incidence rate and nonlinear treatment rate for the control of infectious illness. The incidence rate of infection is considered as Holling type II and the treatment rate is considered as Monod-Haldane (MH) type. The existence and uniqueness criteria for the new model, as well as the non-negativity and boundedness, have been established. We also provide an ideal control strategy for the SIR model using the treatment rate as a control parameter. The solution of the suggested model is approximated using the fractional-order Taylor's method. With the help of MATLAB (2018a), we perform numerical simulations and illustrate the results through graphical representations.

Keywords: SIR model; Monod-Haldane type treatment rate; optimal control; Caputo derivative

AMS 2020 Classification: 92D25; 92D30; 26A33; 49J15; 65L07

1 Introduction

Epidemiology, sometimes compared to the biological study of public health, focuses on the prevalence and underlying causes of infection susceptibility among the general population. The use of mathematical models to study such communicable diseases makes it easier to comprehend how diseases spread, to identify elements that affect transmission for efficient control efforts, and to assess goals and intervention approaches. Systematically introducing deterministic models for infectious illnesses, Kermack and McKendrick [1, 2]. To better understand the process of disease transmission, a number of researchers have investigated various epidemic systems by looking at various models, such as those developed by SI [3], SIS [4], SIR [5–10], SIRS [9], SEIR [11–14], SIQR [15], SEIRV [16, 17]. Infectious disease management has been harder during the last several decades. One of the most important health measures for avoiding infectious diseases is vaccination because of its safety and cost. Indeed, high vaccination rates have resulted in dramatic reductions or even elimination of a variety of infectious illnesses, such as smallpox [18], SARS-CoV-2 infection [19, 20]. In the modeling of infectious illnesses [21–27], the incidence rate is crucial in determining the behavior at phenomena. In 1927, Kermack and Mckendrick [1] proposed the transmission rate as βSI. The interaction effect is a linearly rising count of the amount of pathogens in this incidence rate, which is unsuitable for a vast population. As a result, Capasso and Serio [28] proposed a nonlinear occurrence $g(I)S$ for $g'(I) < 0$ that permits particular "behavioral" effects. With behavioral modifications, Capasso and Serio inspired their approach. The potential damage of infection may become extraordinarily high during times of high occurrence, leading to major behavioral modifications that minimize the actual risk of illness [29]. Goel and Nilam [8], Wei and Chen [30], Capasso et al. [31, 32], Zhang et al. [33], Anderson and May [34], Li et al. [35], including Kumar and Nilam [9, 10]. A few writers [36–38], have drawn attention to the significance of taking nonlinear incidence rates into account when studying the relationships between infectious transmission and illness. Li et al. [35] presented a SIR model with $f(S, I) = \dfrac{\beta SI}{1 + \gamma I}$.

It is well known that treatment rates are crucial in avoiding and limiting the spread of illnesses. We are aware that the therapy resources in any community are insufficient. As a result, selecting an effective treatment rate is critical for limiting disease transmission. Due to a lack of efficient treatment options and vaccinations, epidemic prevention methods focus on efficient preventative measures. Wang and Ruan [39] proposed the following SIR transmission dynamics with a fixed treatment rate:

$$h(I) = \begin{cases} n & \text{for } I > 0, \\ 0 & \text{for } I = 0. \end{cases}$$

Zhang and Liu [40], who also provided a superior treatment rate (Holling type II) as a continuously differentiable function that populates at the largest benefit, as shown below: $h(I) = \frac{mI}{1+nI}$ for $I \geq 0, m > 0, n > 0$, where m represents the cure rate and n represents the limitation rate in treatment availability. Zhang et al. [41], Zhou et al. [42] and Dubey et al. [43] have investigated this nonlinear saturation treatment rate in a somewhat different manner. Kumar [44] proposed a dynamical model of epidemic along with time delay; Holling Type II incidence rate and Monod–Haldane type treatment rate.

Motivation and research background

A particularly useful tool for modelling an infectious disease system that includes past illness states, a memory of past disease patterns, a profile of genetic diversity, etc. is fractional calculus

[45–48]. When compared to an integer order model, using fractional order derivatives to fine-tune complicated dynamics within a disease system produces a more accurate picture. Because it expands the possibilities of integer-order derivatives, fractional-order modelling is a useful tool for analyzing disease features. The integer order derivative is limited to local characteristics, but the fractional order derivative has a broad scope. When the system's consistency domain is improved, the fractional derivative likewise does better. In this paper, three potential categories using the Caputo technique are studied using the fractional order SIR compartmental model with a nonlinear incidence rate and nonlinear treatment rate. The saturated incidence rate of infection is considered as Holling type II and the treatment rate is considered as Monod-Haldane (MH) type. The existence and uniqueness criteria for the new models, as well as the solution's positivity, have been established, among other conclusions. Both at E_0 and E_1, we have covered the stability analysis of our suggested model. For estimating the system solution, Taylor's approach is also used. We used the MATLAB (2018a) program to run numerical simulations and analyze the graphical significance.

Paper structure

Section 2 introduces a pre-requisite concept. We developed the SIR epidemic model in Section 3 in an environment of the Caputo derivative. In Section 4, the model's solution has been examined in terms of its existence, uniqueness, non-negativity, boundedness criteria, and stability analysis. Using the control parameter treatment rate, we also provide an ideal control strategy for a SIR model in Section 5. The suggested model's approximate solution is discussed in Section 6 using the fractional-order Taylor's technique in the Caputo derivative. In Section 7, the MATLAB-based numerical analysis is presented. Section 8 is where the paper comes to a conclusion.

2 Preliminaries

Definition 1 *[49] Let $f \in C^n([t_0, \infty+), \mathbb{R})$, the Caputo derivative of fractional order $\alpha > 0$ is defined by*

$$\begin{matrix} C \\ t_0 \end{matrix} D_t^\alpha f(t) = \frac{1}{\Gamma(n-\alpha)} \int_{t_0}^t \frac{f^{(n)}(s)}{(t-s)^{\alpha-n+1}} ds,$$

where $\Gamma(\cdot)$ represent the Gamma function, $t \geq t_0$, $n \in \mathbb{Z}^+$ and $\alpha \in (n-1, n)$.

Lemma 1 *[50] Consider the system*

$$\begin{matrix} C \\ t_0 \end{matrix} D_t^\alpha u(t) = g(t, x), t_0 > 0,$$

with initial condition $u(t_0) = u_{t_0}$, where $\alpha \in (0, 1]$, $g : [t_0, \infty) \times \Omega \to \mathbb{R}^n, \Omega \in \mathbb{R}^n$, if Lipschitz condition is satisfied by $g(t, x)$ with respect to x, then there exists a solution of (3.2) on $[t_0, \infty) \times \Omega$ which is unique.

Lemma 2 *[51] Let $0 < \alpha \leq 1$, $\phi(t) \in C[a, b]$. If $\begin{matrix} C \\ t_0 \end{matrix} D_t^\alpha f(t) \geq 0 \left(\begin{matrix} C \\ t_0 \end{matrix} D_t^\alpha f(t) \leq 0 \right), t \in (a, b)$ then $\phi(t)$ is a increasing (decreasing) function for $t \in [a, b]$.*

Lemma 3 *[52] The Laplace transform of the Caputo derivative is given by:*

$$\mathscr{L} \left\{ \begin{matrix} C \\ t_0 \end{matrix} D_t^\alpha f(t) \right\} = p^\alpha F(p) - \sum_{j=0}^{n-1} p^{\alpha-j-1} f^j(t_0),$$

where $F(p) = \mathscr{L}\{f(t)\}$.

Lemma 4 *[53] For any $B \in \mathbb{C}^{n \times n}$ where $\mathbb{C}$ be the complex plane and $c, d > 0$, the Laplace transform of Mittag-Leffler function is defined as*

$$\mathscr{L}\left\{t^{d-1}E_{c,d}(Bt^c)\right\} = s^{c-d}(s^c - B)^{-1},$$

for $\mathscr{R}(s) > \|B\|^{\frac{1}{c}}$, where $\mathscr{R}(s)$ denotes the real portion of s.

Lemma 5 *[53] Consider the following fractional-order system:*

$$_{t_0}^{C}D_t^{\alpha}X(t) = \Phi(X), X_{t_0} = (x_{t_0}^1, x_{t_0}^2, ..., x_{t_0}^n), x_{t_0}^i > 0, \quad i = 1, 2, ..., n,$$

with $0 < \alpha \leq 1$, $X(t) = (x^1(t), x^2(t), ..., x^n(t))$ and $\Phi(X) : [t_0, \infty) \to \mathbb{R}^{n \times n}$. The equilibrium points of the above system are evaluated by solving the following system of equations: $\Phi(X) = 0$. These equilibrium points are locally asymptotically stable iff each eigenvalue λ of the Jacobian matrix $J(X) = \dfrac{\partial(\Phi_1, \Phi_2, ..., \Phi_n)}{\partial(x^1, x^2, ..., x^n)}$ calculated at the equilibrium points satisfy $|\arg(\lambda_i)| > \frac{\alpha\pi}{2}$.

Lemma 6 *[54] Suppose $g(t) \in \mathbb{R}_+$ be a differentiable function. Then, for any $t \geq t_0$,*

$$_{t_0}^{C}D_t^{\alpha}\left[g(t) - g^* - g^*\ln\frac{g(t)}{g^*}\right] \leq \left(1 - \frac{g^*}{g(t)}\right) {}_{t_0}^{C}D_t^{\alpha}g(t), \; g^* \in \mathbb{R}_+, \forall \alpha \in (0, 1).$$

Lemma 7 *[54] One parametric and two parametric Mittag-Leffler functions are described as follows:*

$$E_{\alpha}(z) = \sum_{j=0}^{\infty}\frac{z^j}{\Gamma(\alpha j + 1)}, \; and \; E_{a_1, a_2}(z) = \sum_{j=0}^{\infty}\frac{z^j}{\Gamma(a_1 j + a_2)}, \; where \; \alpha, a_1, a_2 \in \mathbb{R}_+.$$

3 Formulation of the model system

We have introduced a mathematical framework that posits the division of the entire population, denoted as N, into three distinct categories: susceptible individuals denoted as S, infected individuals denoted as I, and individuals who have recovered, represented as R at a time t.

The sub-populations at different times may vary, but the total of all sub-populations remains constant, denoted as N. This can be expressed as $S(t) + I(t) + R(t) = N$. The term $\frac{\beta SI}{1+\gamma I}$ is the Holling type II functional response representing the saturated incidence rate of infection among susceptible where β is the transmission rate between susceptible and infected population. Also, the term $\frac{mI}{1+n^2 I}$ represents the Monod-Haldane type treatment rate, which describes the non-monotonic behavior of the treatment rate due to limitations in the availability of effective treatments. Table 1 provides a summary of the symbols used in the proposed model system.

$$
\begin{aligned}
{}_{t_0}^{C}D_t^{\alpha}S(t) &= \Lambda - \mu S(t) - \frac{\beta S(t)I(t)}{1+\gamma I(t)}, \; S(t)|_{t=0} = S(0) > 0, \\
{}_{t_0}^{C}D_t^{\alpha}I(t) &= \frac{\beta S(t)I(t)}{1+\gamma I(t)} - \frac{mI(t)}{1+nI^2(t)} - (\mu + r + \delta)I(t), \; I(t)|_{t=0} = I(0) > 0, \\
{}_{t_0}^{C}D_t^{\alpha}R(t) &= \frac{mI(t)}{1+nI^2(t)} + \delta I(t) - \mu R(t), \; R(t)|_{t=0} = R(0) > 0,
\end{aligned}
\tag{1}
$$

where $0 < \alpha < 1$, and ${}^{C}_{t_0}D^{\alpha}_t$ denotes the Caputo operator.
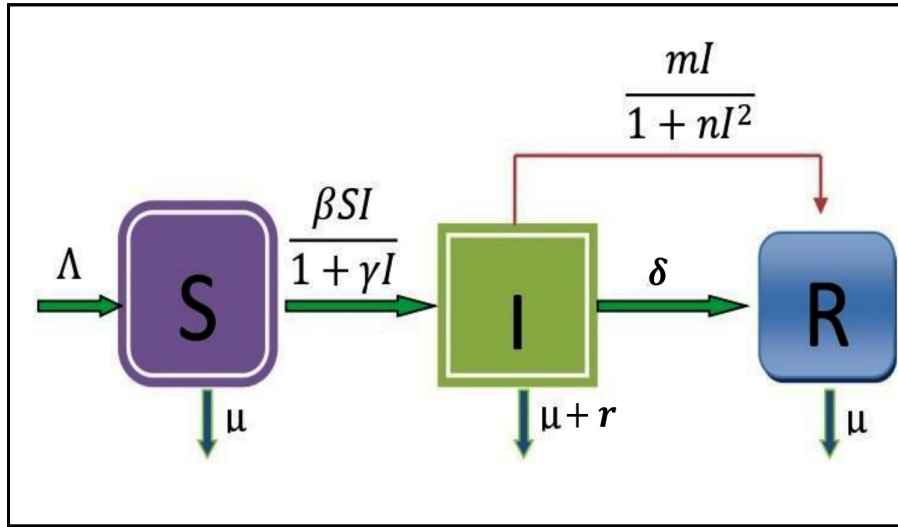
Figure 1. The proposed SIR model's flow diagram

Table 1. Significance of the relevant parameters

Parameters	Biological meaning
Λ	recruitment rate
μ	death rate
β	transmission rate
γ	inhibitory rate
m	treatment rate
n	limitation rate in resources availability
δ	recovery rate
r	disease-induced mortality rate

4 Analysis of the system

Model existence and model uniqueness

Theorem 1 *The model* (1), *with an initial condition of* $(S(t_0), I(t_0), R(t_0))$ *belonging to the positive region* Γ^+, *invariably exhibits a singular solution within the domain* Γ^+ *for all time points* $t \geq t_0$.

Proof Let $\Omega = \{(S, I, R) \in \mathbb{R}^3 : \max(|S|, |I|, |R|) \leq M\}$ where τ and M are finite positive real numbers for the region $\Omega \times [t_0, \tau]$. Let $Y = (S, I, R)$ and $\overline{Y} = (\bar{S}, \bar{I}, \bar{R})$.
Consider a mapping $F(Y) = (F_1(Y), F_2(Y), F_3(Y))$, where

$$F_1(Y) = \Lambda - \mu S(t) - \frac{\beta S(t)I(t)}{1 + \gamma I(t)},$$
$$F_2(Y) = \frac{\beta S(t)I(t)}{1 + \gamma I(t)} - \frac{mI(t)}{1 + nI^2(t)} - (\mu + \delta + r)I(t),$$
$$F_3(Y) = \frac{mI(t)}{1 + nI^2(t)} + \delta I(t) - \mu R(t).$$

For any $Y, \overline{Y} \in \Omega$:

$$\left\| F(Y) - F(\overline{Y}) \right\|$$

$$= \left| F_1(Y) - F_1(\overline{Y}) \right| + \left| F_2(Y) - F_2(\overline{Y}) \right| + \left| F_3(Y) - F_3(\overline{Y}) \right|$$

$$= \left| \Lambda - \mu S - \frac{\beta S I}{1 + \gamma I} - \left(\Lambda - \mu \bar{S} - \frac{\beta \bar{S} \bar{I}}{1 + \gamma \bar{I}} \right) \right|$$

$$+ \left| \frac{\beta S I}{1 + \gamma I} - \frac{m I}{1 + n I^2} - (\mu + \delta + r) I - \left(\frac{\beta \bar{S} \bar{I}}{1 + \gamma \bar{I}} - \frac{m \bar{I}}{1 + n \bar{I}^2} \right) + (\mu + \delta + r) \bar{I} \right|$$

$$+ \left| \frac{m I}{1 + n I^2} + \delta I - \mu R - \left(\frac{m \bar{I}}{1 + n \bar{I}^2} + \delta \bar{I} - \mu \bar{R} \right) \right|$$

$$\leq \mu \left| (S - \bar{S}) \right| + 2\beta \left| \left(\frac{S I}{1 + \gamma I} - \frac{\bar{S} \bar{I}}{1 + \gamma \bar{I}} \right) \right| + 2m \left| \left(\frac{I}{1 + n I^2} - \frac{\bar{I}}{1 + n \bar{I}^2} \right) \right|$$

$$+ (\mu + 2\delta + r) \left| (I - \bar{I}) \right| + \mu \left| (R - \bar{R}) \right|$$

$$\leq \mu \left| (S - \bar{S}) \right| + 2\beta \left| \left(\frac{S I (1 + \gamma \bar{I}) - \bar{S} \bar{I} (1 + \gamma I)}{(1 + \gamma I)(1 + \gamma \bar{I})} \right) \right| + 2m \left| \left(\frac{I(1 + n \bar{I}^2) - \bar{I}(1 + n I^2)}{(1 + n I^2)(1 + n \bar{I}^2)} \right) \right|$$

$$+ (\mu + 2\delta + r) \left| (I - \bar{I}) \right| + \mu \left| (R - \bar{R}) \right|$$

$$\leq \mu \left| (S - \bar{S}) \right| + 2\beta K [M \left| (S - \bar{S}) \right| + \left| (I - \bar{I}) \right| + \gamma M^2 \left| (I - \bar{I}) \right|] + 2m L (1 + n M^2) \left| (I - \bar{I}) \right|$$

$$+ (\mu + 2\delta + r) \left| (I - \bar{I}) \right| + \mu \left| (R - \bar{R}) \right|$$

$$\leq (\mu + 2\beta M K)) \left| (S - \bar{S}) \right| + \left(\mu + 2\delta + r + 2m L (1 + n M^2) + 2\beta K (1 + \gamma M^2) \right) \left| (I - \bar{I}) \right| + \mu \left| (R - \bar{R}) \right|$$

$$\leq G_1 \left| S - \bar{S} \right| + G_2 \left| I - \bar{I} \right| + G_3 \left| R - \bar{R} \right|$$

$$\leq G \left\| Y - \overline{Y} \right\|,$$

where $G = \max\{G_1, G_2, G_3\}$, $G_1 = (\mu + 2\beta M)$, $G_2 = \left(\mu + 2\delta + r + 2m L (1 + n M^2) + 2\beta K (1 + \gamma M^2) \right)$ and $G_3 = \mu$, where $\left| (1 + \gamma I)(1 + \gamma \bar{I}) \right| \geq K$ and $\left| (1 + n I^2)(1 + n \bar{I}^2) \right| \geq L$. Thus, $F(Y)$ satisfies Lipschitz's criteria. So $Y(t)$ is a unique solution of model (1), with the help of Lemma 1.

Boundedness and non-negativity

Theorem 2 *Any solutions originating from the initial condition* $(S(t_0), I(t_0), R(t_0))$ *in model* (1) *are characterized by non-negative values.*

Proof Let $Y(t_0) = (S(t_0), I(t_0), R(t_0)) \in \Gamma_+$ be the initial solution of (1). Firstly, we shall prove that $S(t) \geq 0$ for all $t \geq 0$. For this, we assume that $S(t) \geq 0$ is not true. Then there exists a $\tau_1 > 0$, such that

$$\begin{cases} S(t) > 0 \text{ for } t_0 \leq t < \tau_1, \\ S(t) = 0 \text{ for } t = \tau_1, \\ S(t) < 0 \text{ for } \tau_1 < t < \tau_1 + \epsilon_1 \text{ for } \epsilon_1 > 0. \end{cases}$$

With the help of system (1), we have

$$^C_{t_0} D^\alpha_t S(t) |_{S(\tau_1) = 0} = \Lambda > 0.$$

Using Lemma 2, for any $0 < \epsilon_1 << 1$, we have $S(\tau_1 + \epsilon_1) = S(\tau_1) + \frac{1}{\alpha} \frac{d^\alpha}{dt^\alpha} S(t) \epsilon_1{}^\alpha$. As a result, $S(\tau_1 + \epsilon_1) \geq 0$, contradicts our assumption that $S(t) < 0$ for $\tau_1 < t < \tau_1 + \epsilon_1$. Therefore, we get $S(t) \geq 0, \forall t \in [t_0, \infty)$. Secondly, we shall prove that $I(t) \geq 0$ for all $t \geq 0$. For this, we assume

that $I(t) \geq 0$ is not true. Then there exists a $\tau_2 > 0$, such that

$$
\begin{cases}
I(t) > 0 \text{ for } t_0 \leq t < \tau_2, \\
I(t) = 0 \text{ for } t = \tau_2, \\
I(t) < 0 \text{ for } \tau_2 < t < \tau_2 + \epsilon_2 \text{ for } \epsilon_2 > 0.
\end{cases}
$$

With the help of system (1), we have

$$
{}^{C}_{t_0}D^{\alpha}_{t}I(t)|_{I(\tau_2)=0} = 0.
$$

Using Lemma 2, for any $0 < \epsilon_2 << 1$, we have $I(\tau_2 + \epsilon_2) = I(\tau_2) + \frac{1}{\alpha}\frac{d^{\alpha}}{dt^{\alpha}}I(t)\epsilon_2{}^{\alpha}$. As a result, $I(\tau_2 + \epsilon_2) = 0$, contradicts our assumption that $I(t) < 0$ for $\tau_2 < t < \tau_2 + \epsilon_2$. Therefore, we get $I(t) \geq 0, \forall t \in [t_0, \infty)$. Lastly, we shall prove that $R(t) \geq 0$ for all $t \geq 0$. For this, we assume that $R(t) \geq 0$ is not true. Then there exists a $\tau_3 > 0$, such that

$$
\begin{cases}
R(t) > 0 \text{ for } t_0 \leq t < \tau_3, \\
R(t) = 0 \text{ for } t = \tau_3, \\
R(t) < 0 \text{ for } \tau_3 < t < \tau_3 + \epsilon_3 \text{ for } \epsilon_3 > 0.
\end{cases}
$$

With the help of system (1), we have

$$
{}^{C}_{t_0}D^{\alpha}_{t}R(t)|_{R(\tau_3)=0} = \frac{mI(\tau_3)}{1 + nI^2(\tau_3)} + \delta I(\tau_3) > 0.
$$

Using Lemma 2, for any $0 < \epsilon_3 << 1$, we have $R(\tau_3 + \epsilon_3) = R(\tau_3) + \frac{1}{\alpha}\frac{d^{\alpha}}{dt^{\alpha}}R(t)\epsilon_3{}^{\alpha}$. As a result, $R(\tau_3 + \epsilon_3) \geq 0$, contradicts our assumption that $R(t) < 0$ for $\tau_3 < t < \tau_3 + \epsilon_3$. Therefore, we get $R(t) \geq 0, \forall t \in [t_0, \infty)$.

Theorem 3 *All solutions of system* (1) *are bounded.*

Proof Now $N(t) = S(t) + I(t) + R(t)$, then

$$
\begin{aligned}
{}^{C}_{t_0}D^{\alpha}_{t}N(t) &= {}^{C}_{t_0}D^{\alpha}_{t}S(t) + {}^{C}_{t_0}D^{\alpha}_{t}I(t) + {}^{C}_{t_0}D^{\alpha}_{t}R(t) \\
&= \Lambda - \mu N(t) - rI(t).
\end{aligned}
$$

Therefore,

$$
{}^{C}_{t_0}D^{\alpha}_{t}N(t) + \mu N(t) \leq \Lambda \quad (\text{as } I \geq 0).
$$

We get (using Lemma 3):

$$
\begin{aligned}
z^{\alpha}F(z) - z^{\alpha-1}N(0) + \mu F(z) &\leq \frac{\Lambda}{z}, \text{ where } F(z) = \mathscr{L}\{N(t)\} \\
\Rightarrow F(z)(z^{\alpha+1} + z\mu) &\leq z^{\alpha}N(0) + \Lambda \\
\Rightarrow F(z) &\leq \frac{z^{\alpha}N(0) + \Lambda}{z^{\alpha+1} + z\mu} \\
&= \frac{z^{\alpha}N(0)}{z^{\alpha+1} + z\mu} + \frac{\Lambda}{z^{\alpha+1} + z\mu}.
\end{aligned}
$$

Using inverse Laplace transform:

$$N(t) \leq N(0)E_{\alpha,1}(-\mu t^{\alpha}) + \Lambda t^{\alpha}E_{\alpha,\alpha+1}(-\mu t^{\alpha}).$$

From the properties of Mittag-Leffler function [55], we get

$$E_{c,d}(x) = xE_{c,c+d}(x) + \frac{1}{\Gamma(d)}.$$

Hence,

$$N(t) \leq (N(0) - \frac{\Lambda}{\mu})E_{\alpha,1}(-\mu t^{\alpha}) + \frac{\Lambda}{\mu}.$$

As a result, the system solutions are bounded. It completes the proof of the theorem. The impact of $R(t)$ on the first two equations in system (1) is unaltered. System (1) might be converted to a two-dimensional system on the presumption that the whole population N is constant. The third equation of the system (1) is traditionally omitted. As a result, we have:

$$
\begin{aligned}
{}^{C}_{t_0}D^{\alpha}_t S(t) &= \Lambda - \mu S(t) - \frac{\beta S(t)I(t)}{1 + \gamma I(t)}, \ S(t)|_{t=0} = S(0) > 0, \\
{}^{C}_{t_0}D^{\alpha}_t I(t) &= \frac{\beta S(t)I(t)}{1 + \gamma I(t)} - \frac{mI(t)}{1 + nI^2(t)} - (\mu + r + \delta)I(t), \ I(t)|_{t=0} = I(0) > 0.
\end{aligned}
\tag{2}
$$

Equilibrium points of the model (2)

Let ${}^{C}_{t_0}D^{\alpha}_t S(t) = 0$ and ${}^{C}_{t_0}D^{\alpha}_t I(t) = 0$. The model (2) has two equilibrium points namely,

i. The infection free equilibrium is $E_0(\frac{\Lambda}{\mu}, 0)$.
ii. The endemic equilibrium is $E_1(S^*, I^*)$, where
$S^* = \frac{\Lambda + I^*(-m - \mu - \delta - r) + I^{*2}(\Lambda n) - n(\mu + \delta + r)I^{*3}}{\mu(1 + nI^{*2})}$ and $XI^{*3} + YI^{*2} + ZI^* + W = 0$, where $X = n(\mu\gamma + \beta)(\mu + \delta + r)$, $Y = \mu n(\mu + \delta + r) - \beta\Lambda n$, $Z = (\mu\gamma + \beta)(m + \mu + \delta + r)$ and $W = \mu(\mu + m + \delta + r) - \Lambda\beta$.

The basic reproduction number

The next-generation matrix [56] technique is used to calculate the model's basic reproduction number R_0, which may be determined from the biggest eigenvalue of the matrix FV^{-1} where,

$$F = \begin{bmatrix} \frac{\beta\Lambda}{\mu} & 0 \\ 0 & 0 \end{bmatrix}, \quad \text{and} \quad V = \begin{bmatrix} m + \mu + \delta + r & 0 \\ \frac{\beta\Lambda}{\mu} & \mu \end{bmatrix}.$$

Therefore, $R_0 = \frac{\beta\Lambda}{\mu(m + \mu + \delta + r)}$.

Stability analysis at E_0

Let us consider $J_0(S, I) = F$ where,

$$F = \begin{bmatrix} F_{11} & F_{12} \\ 0 & F_{22} \end{bmatrix},$$

where

$$F_{11} = -\mu, F_{22} = -(m + \mu + \delta + r), F_{12} = -\frac{\beta\Lambda}{\mu}.$$

Theorem 4 *The point E_0 of system (2) is locally asymptotically stable.*

Proof At E_0 the Jacobian matrix is given by

$$J_0(\frac{\Lambda}{\mu}, 0) = \begin{bmatrix} -\mu & -\frac{\beta\Lambda}{\mu} \\ 0 & -(m + \mu + \delta + r) \end{bmatrix}.$$

The eigenvalues of the system are $\lambda_1 = -\mu, \lambda_2 = -(m + \mu + \delta + r)$. It follows that $|\arg(\lambda_i)| = \pi > \frac{\alpha\pi}{2}$ $(i = 1, 2)$ where $0 < \alpha < 1$. Therefore E_0 is asymptotically stable locally by Lemma 5.

To discuss the global stability at E_0 of system (2), first we assume that $G((S(t), I(t)) = \frac{\beta S(t)I(t)}{1+\gamma I(t)}$, is always positive, monotonically increasing and continuously differentiable for all $S > 0$ and $I > 0$. That satisfies the following conditions [9, 57]:

$C1 : G((S(t), I(t)) > 0, G'_S((S(t), I(t)), G'_I((S(t), I(t))$ for $S > 0$ and $I > 0$.

$C2 : G((S(t), 0) = G((0, I(t)) = 0, G'_S((S(t), 0) = 0, G'_I((S(t), 0) > 0$ for $S > 0$ and $I > 0$.

$C3 : G'_I((S(t), 0)$ is increasing with respect to $S(t) > 0$.

$C4 : \frac{G'_S((S_0, 0)}{G'_I((S(t), 0)} < 1$ for $S(t) > S_0$; $\frac{G'_S((S_0, 0)}{G'_I((S(t), 0)} > 1$ for $S(t) \in (0, S_0)$.

Theorem 5 *Suppose that (C1) to (C4) are satisfied, the point E_0 of system (2) is globally asymptotically stable.*

Proof Let L be the Lyapunov function defined as:

$$L = (S - S_0 - \int_{S_0}^{S} \lim_{t \to 0^+} \frac{G(S_0, I)}{G(g, I)} dg) + I.$$

The aforementioned function's time derivative is

$$\begin{aligned}
{}_{t_0}^{C}D_t^{\alpha} L &= (1 - \frac{S}{S_0}){}_{t_0}^{C}D_t^{\alpha}S + {}_{t_0}^{C}D_t^{\alpha}I \\
&= -\frac{\mu(S - S_0)^2}{S} + \frac{\beta S_0 I}{1 + \gamma I} - \frac{mI}{1 + nI^2} - (\mu + \delta + r)I \\
&\quad -\frac{\mu(S - \frac{\Lambda}{\mu})^2}{S} + \frac{(\mu + \delta + r + m)(R_0 - 1)I}{1 + \gamma I} \\
&\quad -\frac{[-\gamma(\mu + \delta + r + m) + mnI - n\gamma(\delta + r + m)I^2]I^2}{(1 + \gamma I)(1 + nI^2)}.
\end{aligned}$$

Since all parameters of the system are positive, then $^{C}_{t_0}D^{\alpha}_t L \leq 0$ if $R_0 \leq 1$ and $^{C}_{t_0}D^{\alpha}_t L = 0$ if $S = S_0 = \frac{\Lambda}{\mu}, I = I_0 = 0$. The point E_0 is asymptotically stable globally.

Stability analysis at E_1

At $E_1(S^*, I^*)$, we get

$$J(S^*, I^*) = \begin{bmatrix} E & F \\ G & H \end{bmatrix},$$

where

$$E = -\mu - \frac{\beta I^*}{1 + \gamma I^*},$$
$$F = -\frac{\beta S^*}{(1 + \gamma I^*)^2},$$
$$G = \frac{\beta I^*}{(1 + \gamma I^*)},$$
$$H = \frac{\beta S^*}{(1 + \gamma I^*)^2} - \frac{m(1 - nI^{*2})}{(1 + nI^{*2})^2} - (\mu + \delta + r).$$

Theorem 6 *The point $E_1(S^*, I^*)$ of system* (2) *is asymptotically stable locally.*

Proof The characteristic equation is $\lambda^2 + (E + H)\lambda + (EH - FG) = 0$. We have $-(E + H) < 0$ and the roots of the characteristic equation are

$$\lambda_{1,2} = \frac{-(E + H)}{2} \pm \frac{\sqrt{(E + H)^2 - 4(EH - FG)}}{2}.$$

If $EH > FG$ then $\left|\arg(\lambda_{1,2})\right| = \pi > \frac{\alpha\pi}{2}; 0 < \alpha < 1$, since $(E + H)^2 - 4(EH - FG) = (E - H)^2 + 4FG$. Using Lemma 5, the point E_1 is locally asymptotically stable in SI plane.

Theorem 7 *The point $E_1(S^*, I^*)$ of system* (2) *is globally asymptotically stable.*

Proof Let us consider the following hypothesis:

$$H(1) \quad : \quad \frac{mI^*}{1 + nI^{*2}} + \frac{(1 + I)\beta S^* I^*}{1 + I\gamma I^*} + \frac{m}{1 + nI^{*2}}$$
$$\leq [\frac{mI}{1 + nI^2} + \frac{\beta S^{*2}}{S + S\gamma I^*} + I^*(\frac{S\beta}{1 + \gamma} + \frac{m}{1 + nI^2 I^{*2}})].$$

Since (S^*, I^*) is the endemic equilibrium point of model (2), then

$$\Lambda - \mu S^* = \frac{\beta S^* I^*}{1 + \gamma I^*}, \frac{\beta S^* I^*}{1 + \gamma I^*} = \frac{mI^*}{1 + nI^{*2}} + (\mu + \delta + r)I^*. \tag{3}$$

Let us consider the Goh-Volterra form as

$$W(S, I) = \left(S - S^* - S^* \ln \frac{S}{S^*}\right) + \left(I - I^* - I^* \ln \frac{S}{S^*}\right). \tag{4}$$

Now, along the integral curves of (2):

$$
\begin{aligned}
{}^{C}_{t_0}D^{\alpha}_t W(S,I) \;\; &\leq \;\; \frac{S-S^*}{S}\,{}^{C}_{t_0}D^{\alpha}_t S(t) + \frac{I-I^*}{I}\,{}^{C}_{t_0}D^{\alpha}_t I(t) \quad \text{(using Lemma 6)}\\
&= \;\; \frac{mI^*}{1+nI^{*2}} + \frac{(1+I)\beta S^* I^*}{1+I\gamma I^*} + \frac{m}{1+nI^{*2}}\\
&\quad -\Big[\frac{mI}{1+nI^2} + \frac{\beta S^{*2}}{S+S\gamma I^*} + I^*\Big(\frac{S\beta}{1+\gamma} + \frac{m}{1+nI^2 I^{*2}}\Big)\Big] \quad \text{(using (4)).}
\end{aligned}
$$

Hence, by $H(1)$, we have

$$
{}^{C}_{t_0}D^{\alpha}_t W(S,I) \leq 0,\, \forall (S,I) \in \Omega, \tag{5}
$$

and ${}^{C}_{t_0}D^{\alpha}_t W(S,I) = 0$ if $(S,I) = (S^*,I^*)$. So, the point $E_1(S^*,I^*)$ is globally asymptotically stable.

5   SIR model with optimal control

One of the most important tools in the fight against infectious illnesses is the treatment rate. On the subject of optimal control theory in fractional derivatives, Ding et al. [58] and Agarwal et al. [59] have contributed. The fractional optimum control principle is fundamentally challenged by Pontryagin's maximum principle [60]. Our goal is to utilize the control measure v ($0 \leq v(t) \leq 1$) to account for the value of immunization and to choose the optimum control $v*$ to reduce the cost function $J(v)$ of the control strategy. The cost function:

$$
J(v^*) = \; min\;(J(v(t)))\; with\; J(v) = \left(\int_0^{t_f} [I + A_1 v^2]\,dt\right), \tag{6}
$$

subject to

$$
\begin{aligned}
{}^{C}_{t_0}D^{\alpha}_t S(t) &= \Lambda - \mu S(t) - \frac{\beta S(t)I(t)}{1+\gamma I(t)}, S(0) > 0,\\
{}^{C}_{t_0}D^{\alpha}_t I(t) &= \frac{\beta S(t)I(t)}{1+\gamma I(t)} - \frac{vI(t)}{1+nI^2(t)} - (\mu+\delta+r)I(t), I(0) > 0,\\
{}^{C}_{t_0}D^{\alpha}_t R(t) &= \frac{vI(t)}{1+nI^2(t)} + \delta I(t) - \mu R(t), R(t)|_{t=0} = R(0) > 0,
\end{aligned} \tag{7}
$$

where $0 \leq v(t) \leq 1$.

Theorem 8 *Let $v(t)$ be a measurable control function on $[0,t_f]$, with $v(t) \in [0,1]$. Then there exists an optimal control v^* to minimize $J(v)$ of (6) with $v^*=max\,[min(\overline{v},1),0]$, $\overline{v} = \dfrac{(\epsilon_2-\epsilon_3)I}{2A_1(1+nI^2)}$.*

Proof The following method has been used to study the Hamiltonian:

$$
\begin{aligned}
H \;=\;& [I + A_1 v^2] + \epsilon_1\Big(\Lambda - \mu S(t) - \frac{\beta S(t)I(t)}{1+\gamma I(t)}\Big) + \epsilon_2\Big(\frac{\beta S(t)I(t)}{1+\gamma I(t)} - \frac{vI(t)}{1+nI^2(t)} - (\mu+\delta+rI(t))\Big)\\
&+\; \epsilon_3\Big(\frac{vI(t)}{1+nI^2(t)} + \delta I(t) - \mu R(t)\Big),
\end{aligned}
$$

with adjoint variables $\epsilon_i(t), i = 1, 2, 3$ expressed as:

$$
\begin{aligned}
{}^{RL}_{t_0}D^\alpha_t \epsilon_1(t)(t) &= -\frac{\partial H}{\partial S} = -\epsilon_1(-\mu S(t) - \frac{\beta I}{1+\gamma I}) - \epsilon_2 \frac{\beta I}{1+\gamma I}, \\
{}^{RL}_{t_0}D^\alpha_t \epsilon_2(t)(t) &= -\frac{\partial H}{\partial I} = -1 - \epsilon_1(-\frac{\beta S}{(1+\gamma I)^2}) - \epsilon_2(-\frac{\beta S}{(1+\gamma I)^2} - \frac{v(1-nI^2)}{(1+nI^2)^2} \\
&\quad - (\mu + \delta + r)) - \epsilon_3(\frac{v(1-nI^2)}{(1+nI^2)^2} + \delta), \\
{}^{RL}_{t_0}D^\alpha_t \epsilon_3(t)(t) &= -\frac{\partial H}{\partial R} = \epsilon_3 \mu.
\end{aligned}
$$

As a result, the issue of decreasing the Hamiltonian with regard to the control is now the problem of finding $v*$ that minimizes H in the context of (7). The Pontryagin principle is then used to produce the following ideal circumstance:

$$
\frac{\partial H}{\partial v} = 2A_1 v + (\epsilon_2 - \epsilon_3)(\frac{I}{1+nI^2}).
$$

It may be solved with adjoint variables and state variables to produce:

$$
\overline{v} = \frac{(\epsilon_2 - \epsilon_3)I}{2A_1(1+nI^2)}.
$$

Consider the control restrictions and the sign of the function $\frac{\partial H}{\partial v}$ for the best control v^*. As a result, we get

$$
v^* = \begin{cases} 0 & if \quad \frac{\partial H}{\partial v} < 0, \\ \overline{v} & if \quad \frac{\partial H}{\partial v} = 0, \\ 1 & if \quad \frac{\partial H}{\partial v} > 0. \end{cases}
$$

The ideal circumstance for the model system may be obtained by applying $v*$ to the equation above (7).

6 Numerical procedure

The model system (2), as stated in Theorem 1, has a single solution. Taylor's theorem will be used to find the model's numerical solution [60]. Then,

$$
{}^{C}_{t_0}D^\alpha_t S(t) = u_1(t, S, I), S(0) = S_0, t > 0. \tag{8}
$$

Consider the set of points $[0, A]$ as the points on which we are prepared to approximate the system's solution. Actually, we are unable to calculate $S(t)$, which will be the system's necessary solution. We divide $[0, A]$, into P subintervals $[t_j, t_{j+1}]$ of length, i.e., $w = \frac{A}{P}$, using the nodes $t_j = jw$, for $j = 0, 1, 2, ..., P$. We extend the Taylor's theorem at about $t = t_0$, we have a constant $k \in [0, A]$, so that

$$
S(t) = S(t_0) + {}^{C}_{t_0}D^\alpha_t S(t)\left\{\frac{w^\alpha}{\Gamma(\alpha+1)}\right\} + {}^{C}_{t_0}D^{2\alpha}_t[S(t)]_{t=k}\left\{\frac{w^{2\alpha}}{\Gamma(2\alpha+1)}\right\}.
$$

Now substitute ${}^{C}_{t_0}D^\alpha_t S(t) = u_1(t_0, S(t_0), I(t_0))$ and $t = t_0$ in the above equation which provides

$$
S(t_1) = S(t_0) + u_1(t_0, S(t_0), I(t_0))\left\{\frac{w^\alpha}{\Gamma(\alpha+1)}\right\} + {}^{C}_{t_0}D^{2\alpha}_t[S(t)]_{t=k}\left\{\frac{w^{2\alpha}}{\Gamma(2\alpha+1)}\right\}.
$$

If m is small, we ignore the higher terms, then

$S(t_1)=S(t_0)+u_1(t_0,S(t_0),I(t_0))\left\{\dfrac{w^\alpha}{\Gamma(\alpha+1)}\right\}$. A general formula of expanding about $t_j=t_j+w$, provides

$S(t_j+1)=S(t_j)+u_1(t_j,S(t_j),I(t_j))\left\{\dfrac{w^\alpha}{\Gamma(\alpha+1)}\right\}.$

Similarly, we have

$I(t_j+1)=I(t_j)+u_1(t_j,S(t_j),I(t_j))\left\{\dfrac{w^\alpha}{\Gamma(\alpha+1)}\right\}.$

7 Numerical discussion

In this part, we evaluate and verify the analytic results of our model system (1) using detailed numerical simulations. Although the majority of fractional order differential equations lack accurate analytic solutions, approximation, and numerical methods have been devised. Through the mathematical software MATLAB (2018a), we have employed Taylor's theorem in the numerical scheme. Following are several categories for the numerical output of model simulations and the accompanying findings:

Table 2. Parameter values for numerical study

Parameters	Values	Reference
Λ	5	Estimated
μ	0.05	Assumed
β	0.003	Assumed
γ	0.06	Assumed
m	0.03	Assumed
n	0.04	Assumed
δ	0.002	Assumed
r	0.02	Assumed

Case 1: Dynamical features of the whole population for different fractional orders The parameters' values in Table 2 are used to examine people's dynamic behaviour. All individuals' behaviour over time for different fractional orders α is shown in Figure 2 through Figure 4. The number of susceptible people rises as α moves from 0.90 to 0.98, as seen in Figure 2. The number of infected people rises over time as α rises, as seen in Figure 3. When α in Figure 4 goes from 0.90 to 0.98, there are more people who have been found.

Case 2: Stability analysis of the proposed model Figure 5 to Figure 7 depicts the global stability of system (1) at E_1 with different initial condition taking α=0.90, 0.94, 0.98, confirming our theoretical results in Theorem 6. **Case 3: Impact of α on S and I** Figure 8 and Figure 9 show the effects of α on susceptible and infected people. It can be shown from Figure 8 that the number of susceptible persons rises as α increases. Figure 9 shows that the number of infected people first declines but then rises over time.

Case 4: Mean density of S and I under γ values Plotting the mean densities of S and I with respect to γ for different fractional orders is shown in Figure 10 and Figure 11. As seen in Figure 10, the mean density of susceptible people rises as the value of α rises. Figure 11 shows that as the values of α fall, the mean density of infected people rises with regard to γ.

Case 5: Mean density of S and I under δ values Figure 12 and Figure 13 shows the plot of mean density of S and I with respect to δ for various fractional order. Figure 12 shows that the mean density of susceptible people rises as the value of α rises. Figure 13 shows that as the values of α decline, the mean density of infected people rises with regard to δ.
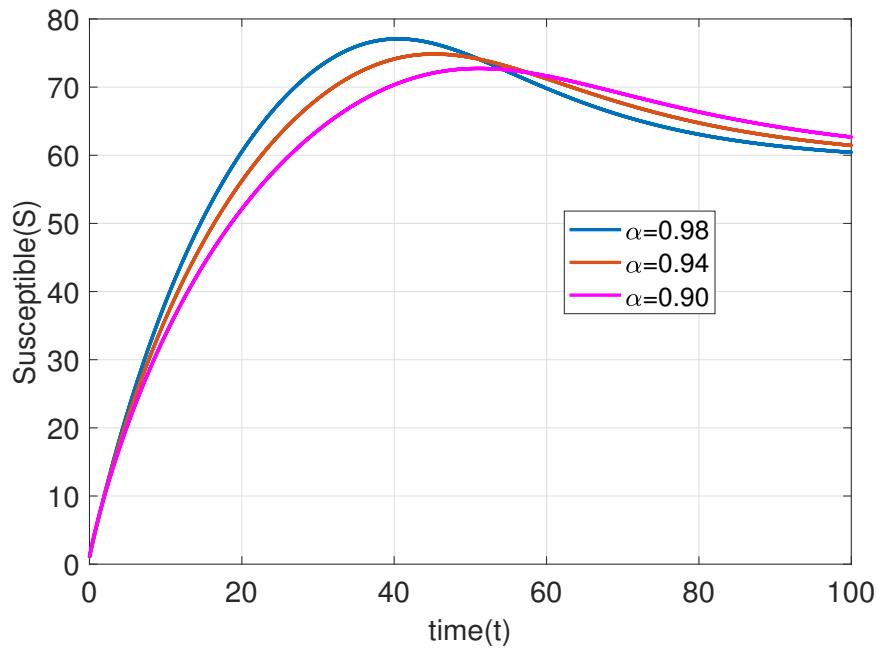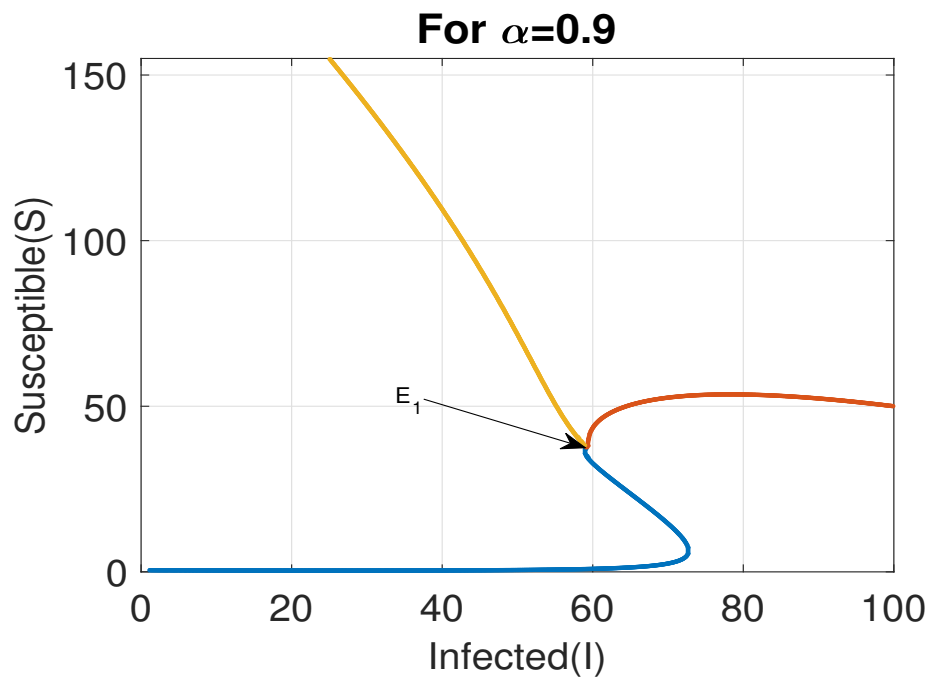
Figure 2. The behavior of Susceptible individuals for values of $\alpha = 0.90, 0.94, 0.98$
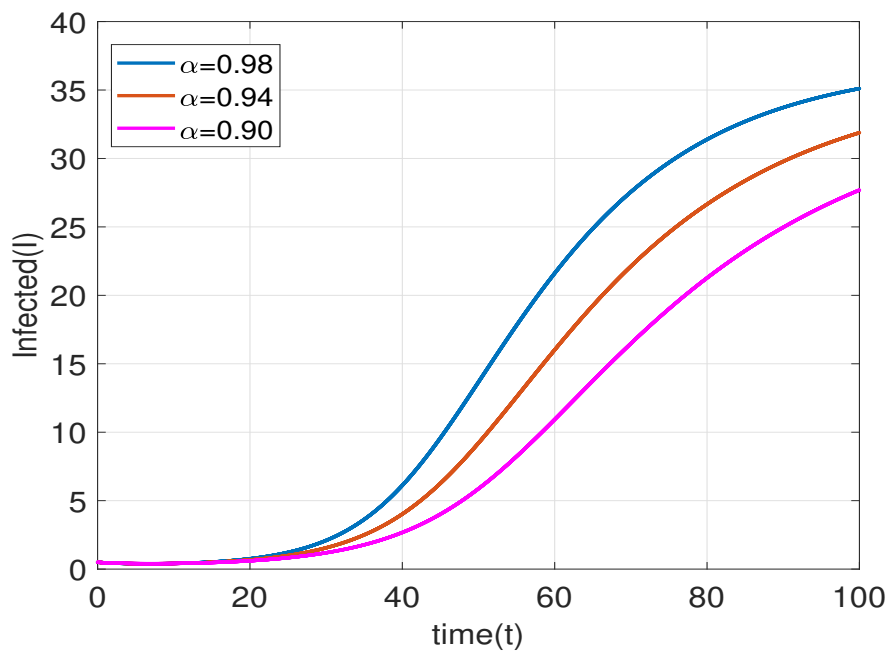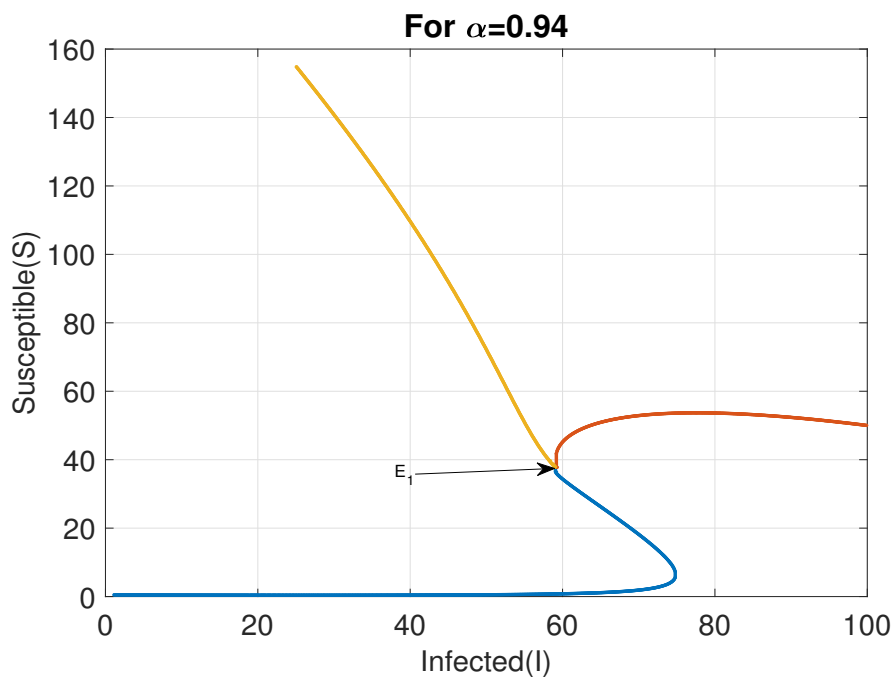
Figure 3. The behavior of Infected individuals for values of $\alpha = 0.90, 0.94, 0.98$
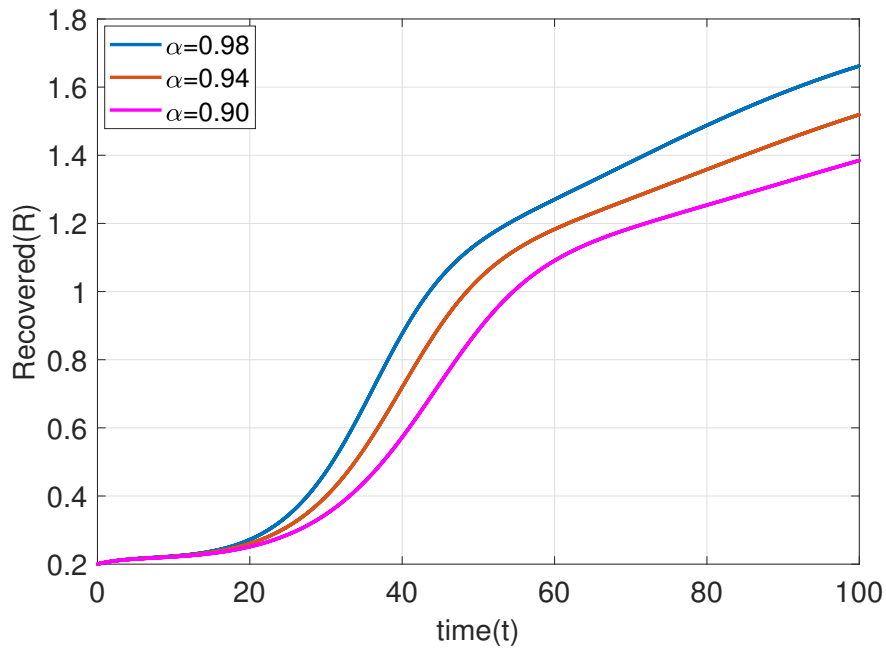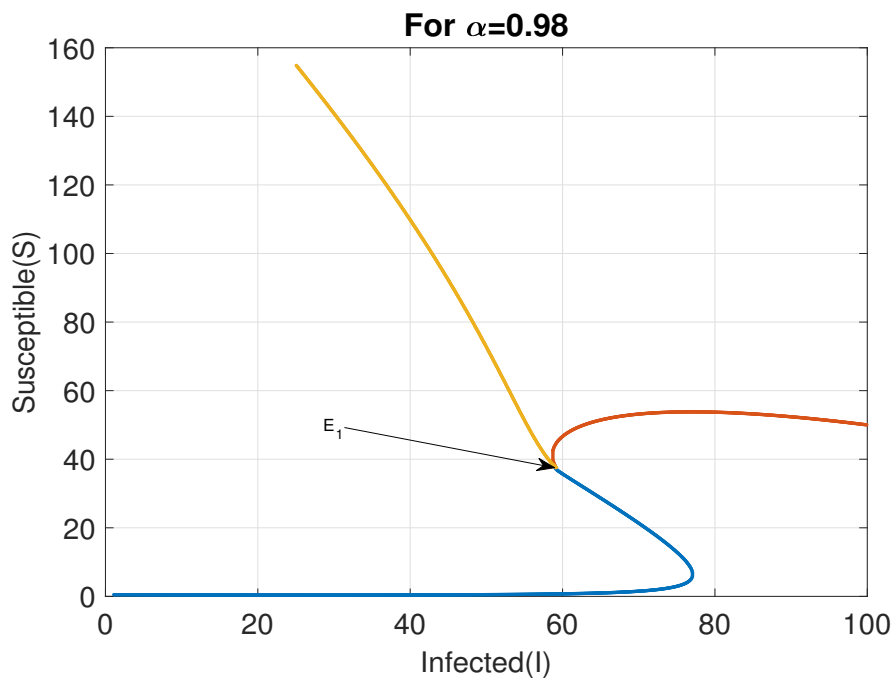
Figure 4. The behavior of Recovered individuals for values of α = 0.90, 0.94, 0.98

Figure 5. Phase portrait diagram for values of α = 0.90
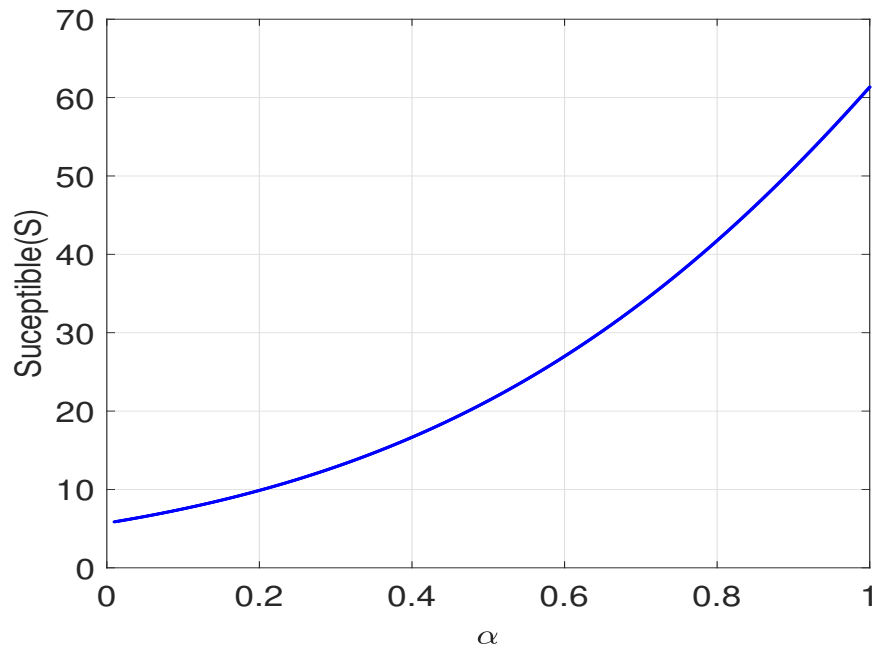
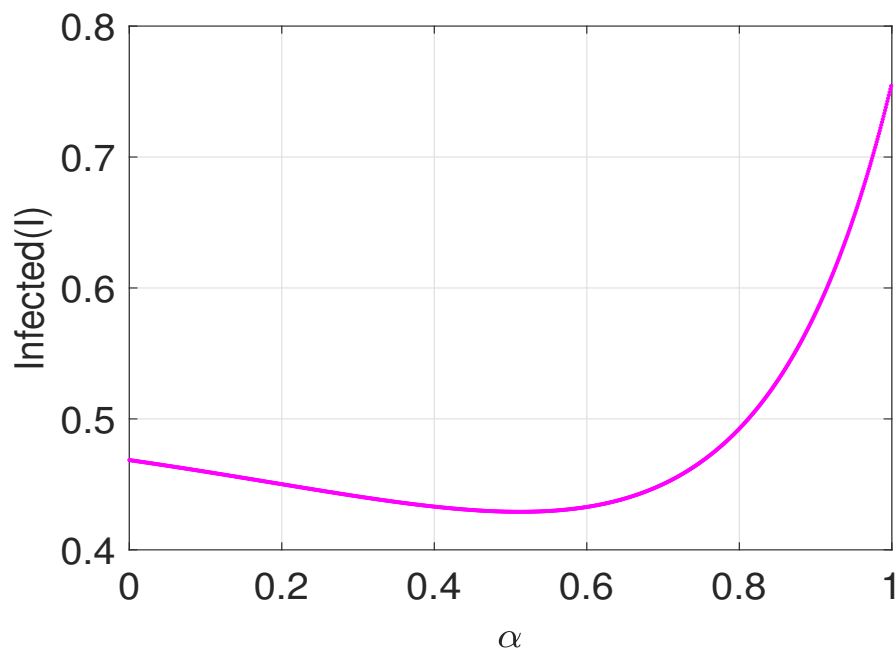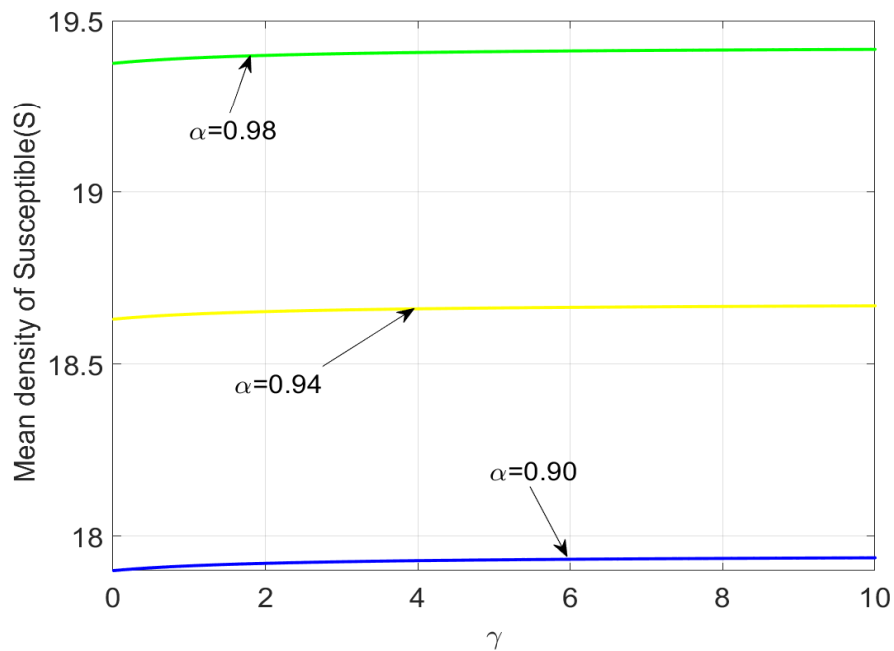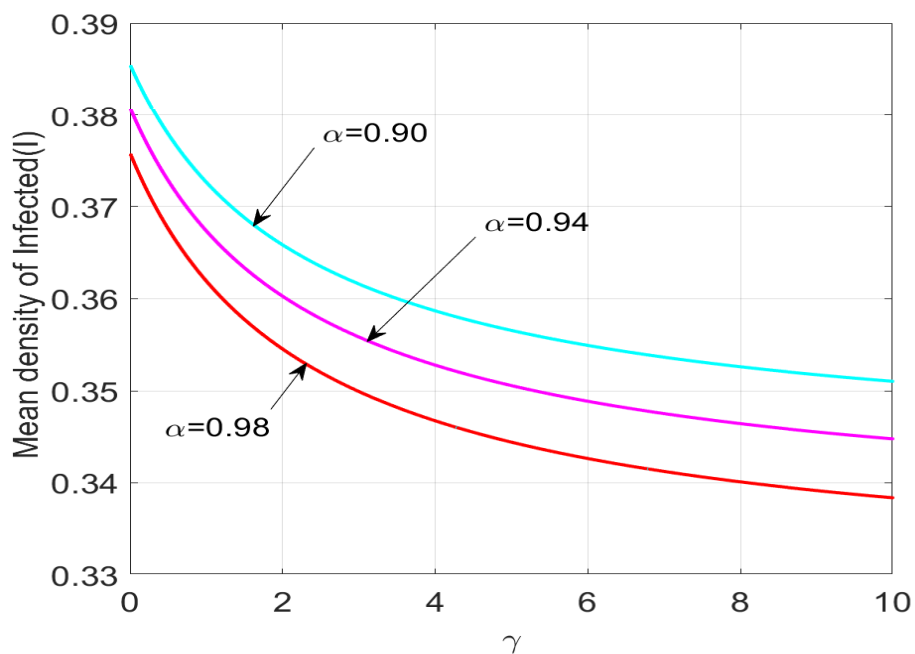**Figure 6.** Phase portrait diagram for values of $\alpha = 0.94$

Figure 7. Phase portrait diagram for values of $\alpha = 0.98$

Figure 8. Dynamics of S under α values

Figure 9. Dynamics of I under α values

Figure 10. Mean density of *S* under γ for $\alpha = 0.90, 0.94, 0.98$

Figure 11. Mean density of *I* under γ for $\alpha = 0.90, 0.94, 0.98$
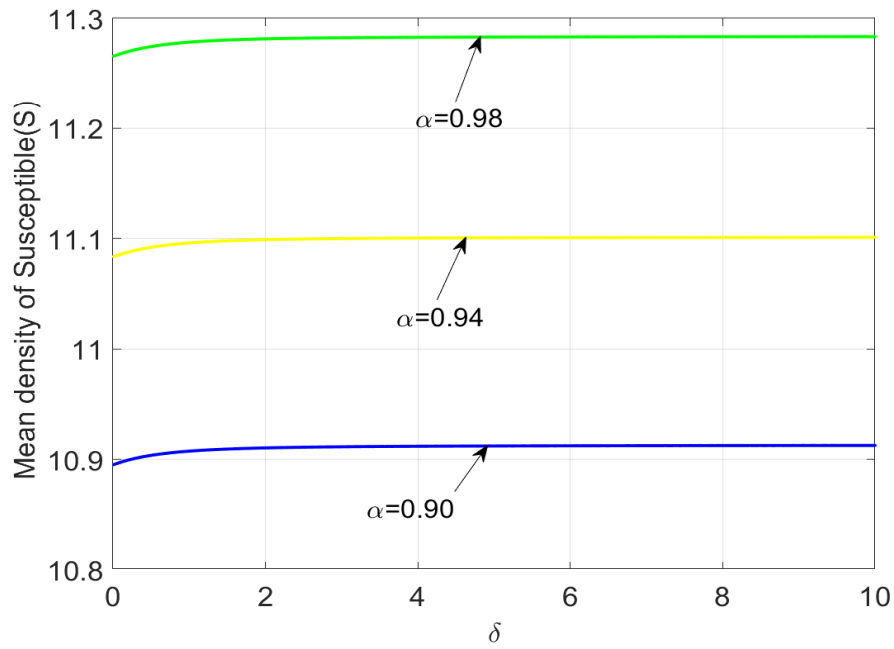
Figure 12. Mean density of *S* under δ for α=0.90, 0.94, 0.98
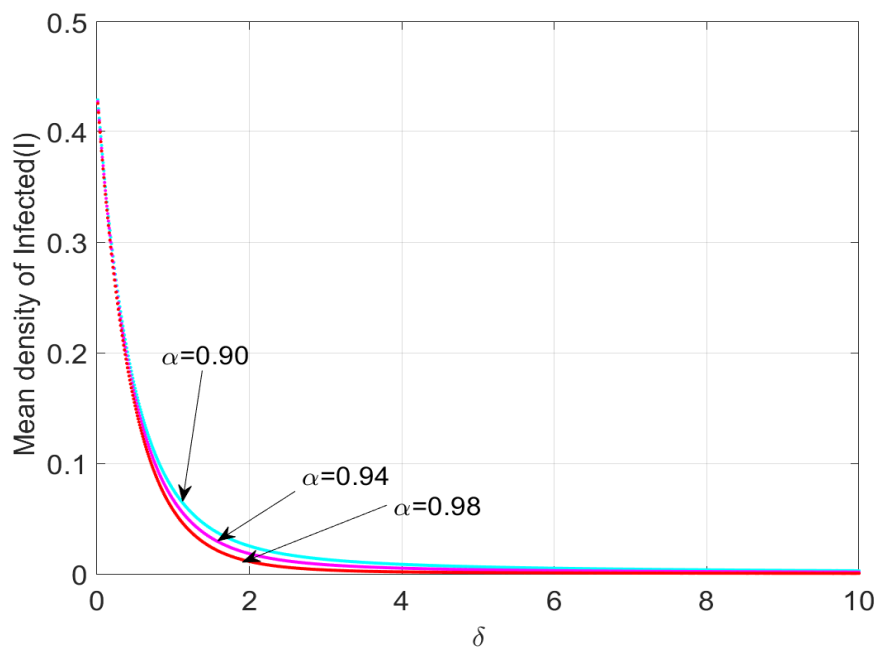
Figure 13. Mean density of *I* under δ for α = 0.90, 0.94, 0.98

Case 6: Variation of γ **under** *S* **and** *I* **for** α = 0.98 Figure 14 and Figure 15 shows that the effect of γ on *S* and *I* with time for α=0.98. Figure 14 demonstrates a rise in the number of vulnerable people as the inhibitory rate γ drops and reaches its stable state, but the illness is not completely eradicated since it will continue to exist at a much lower level. We noticed that the infected population drops when the inhibitory rate γ rises in Figure 15. Thus, it is assumed that preventative actions conducted by vulnerable and sick individuals will aid in reducing the spread of illness.
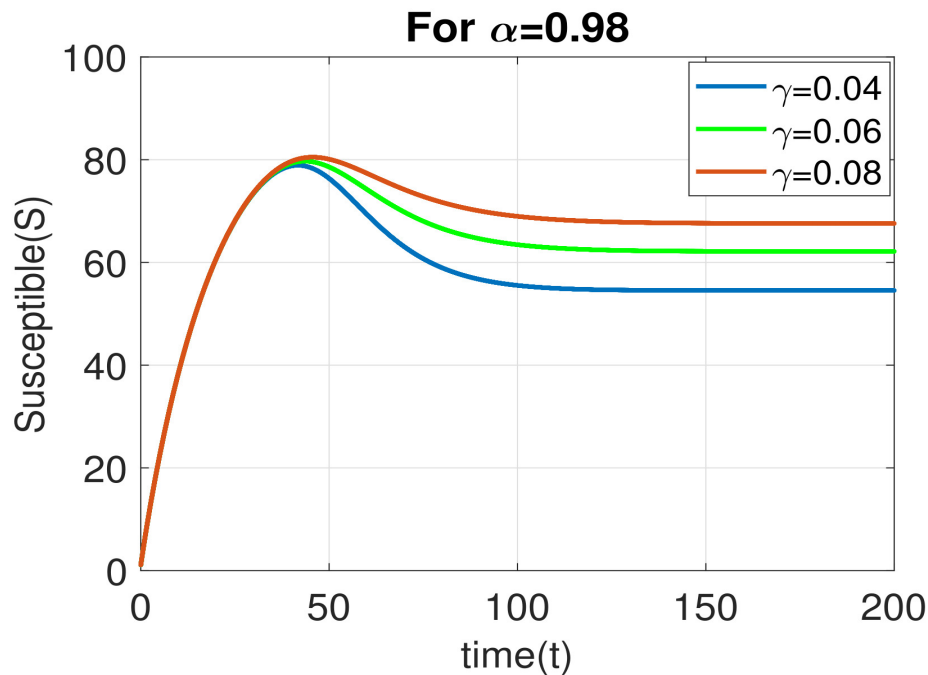

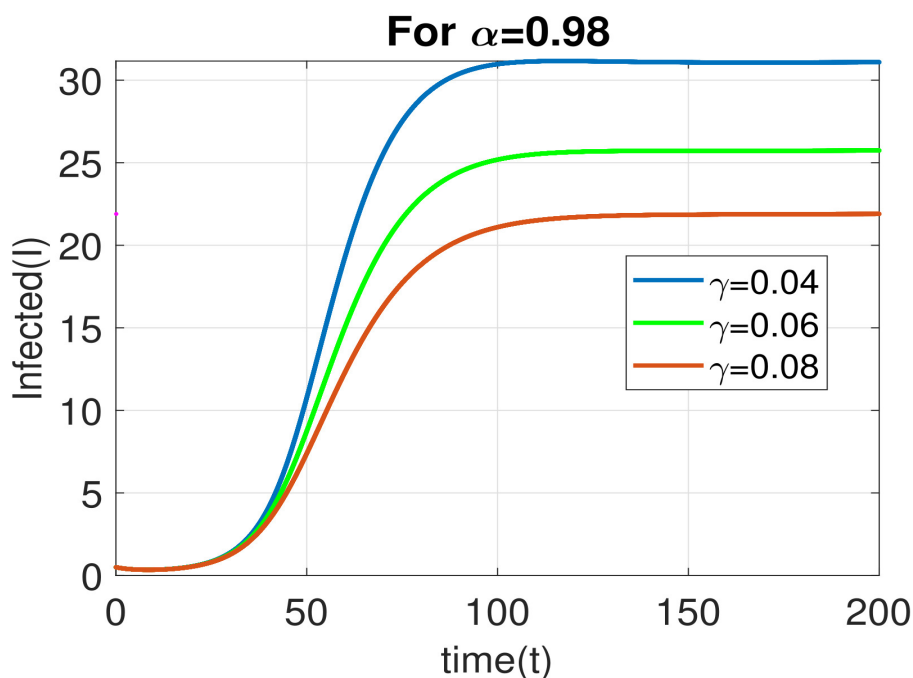**Figure 14.** Variation of γ under *S* for α=0.98

Figure 15. Variation of γ under *I* for α=0.98

Case 7: Variation of δ under S and I for α=0.98. Figure 16 and Figure 17 shows that the effect of δ on S and I with time for α=0.98. As the recovery rate δ declines and reaches its steady state, Figure 16 depicts a rise in the number of sensitive people. In Figure 17, we observed that the infected population decreases when the recovery rate δ changes from 0.001 to 0.003.
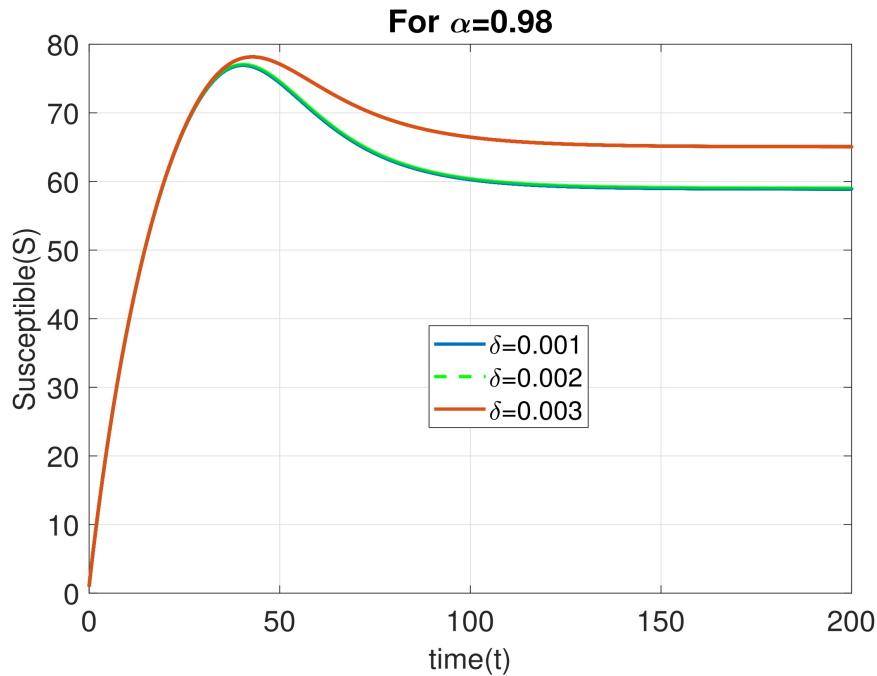

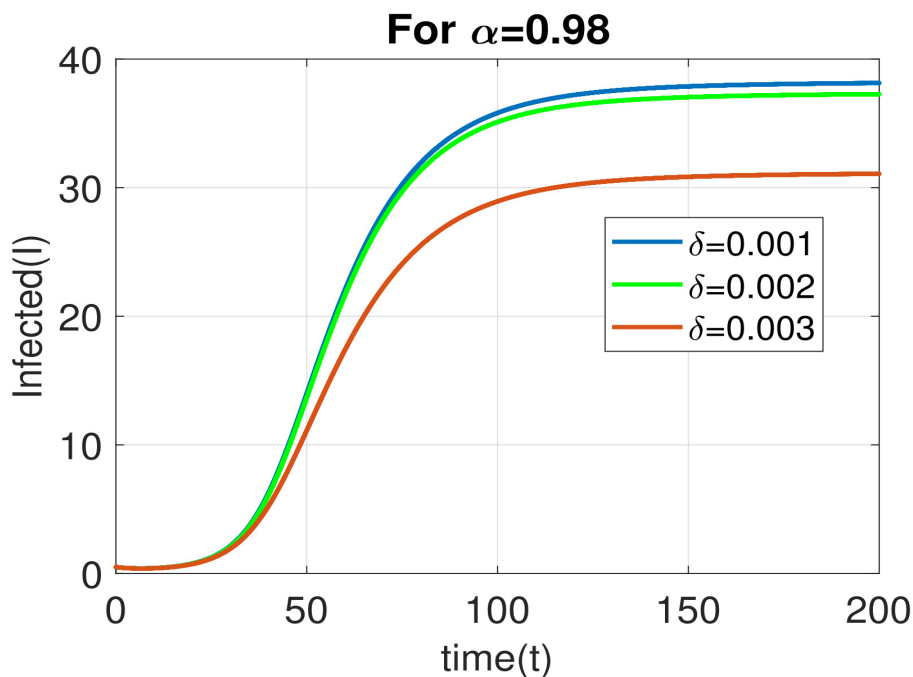**Figure 16.** Variation of δ under S for α=0.98


**Figure 17.** Variation of δ under I for α=0.98

Case 8: Optimal control Figure 18 and Figure 19 depict the time series of people who are vulnerable to infection, those who have been infected, and those who have recovered over a time period of $[0, 100]$, with optimum control using fractional order $\alpha=0.9$. Infectious illness prevention depends heavily on treatment rates, and several theories have been put out in which vaccination rates are seen as very advantageous. The reproduction number R_0 falls as a consequence of the inclusion of the treatment rate parameter. We chose a final time of $t_f=100$ for the simulation of the optimum control problem governed by model (1), which corresponds to Table 2. The time series of the ideal cost J^* and the ideal control variable v^* are shown in Figure 20 and Figure 21.
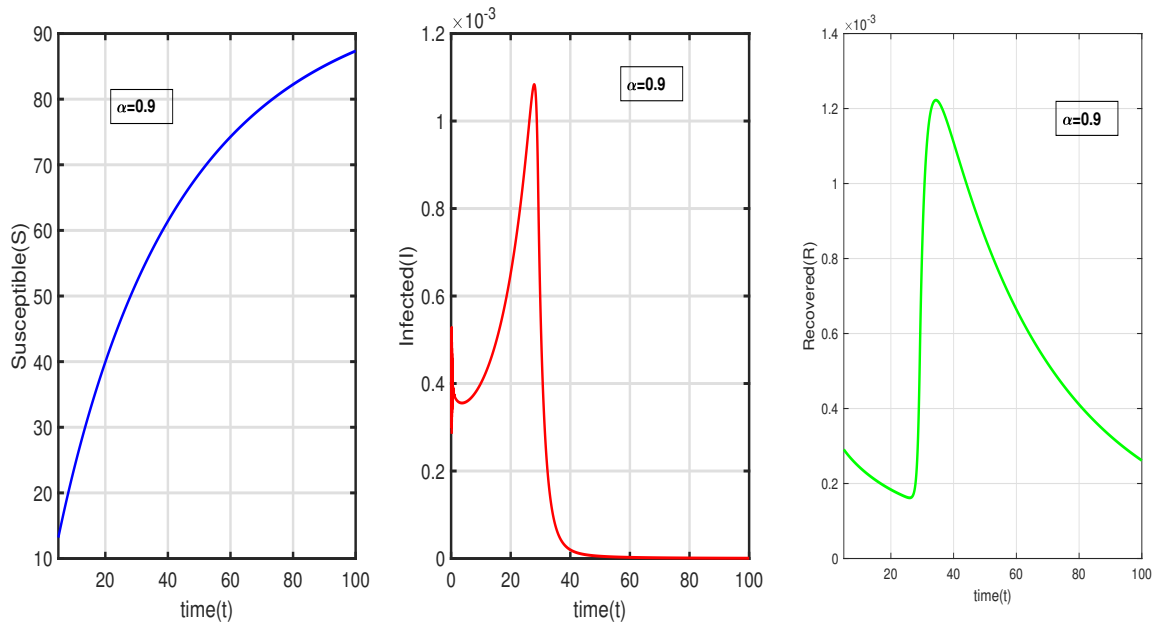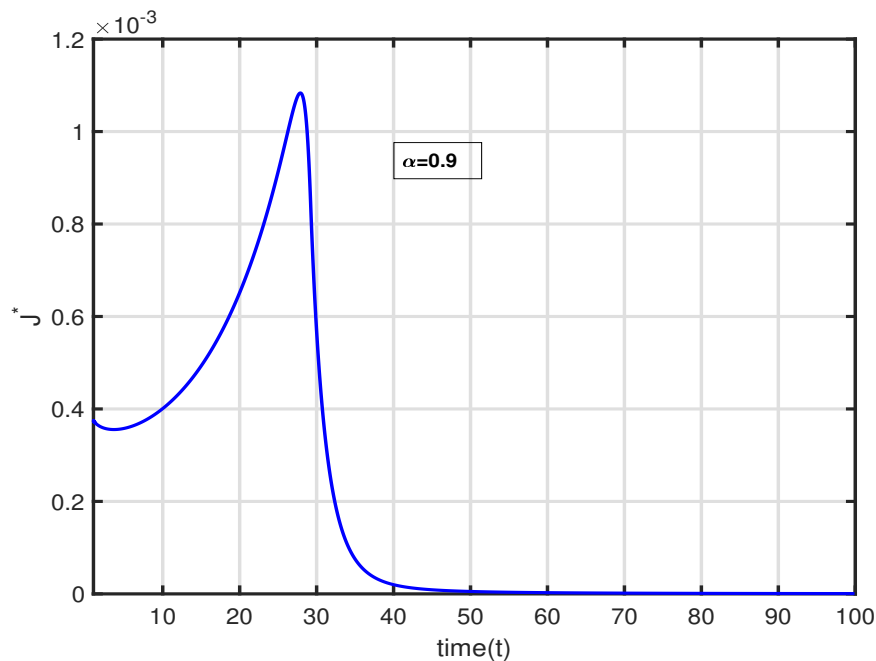

Figure 18. When $\alpha=0.9$, the time series of the model system (1) corresponds to Table 2
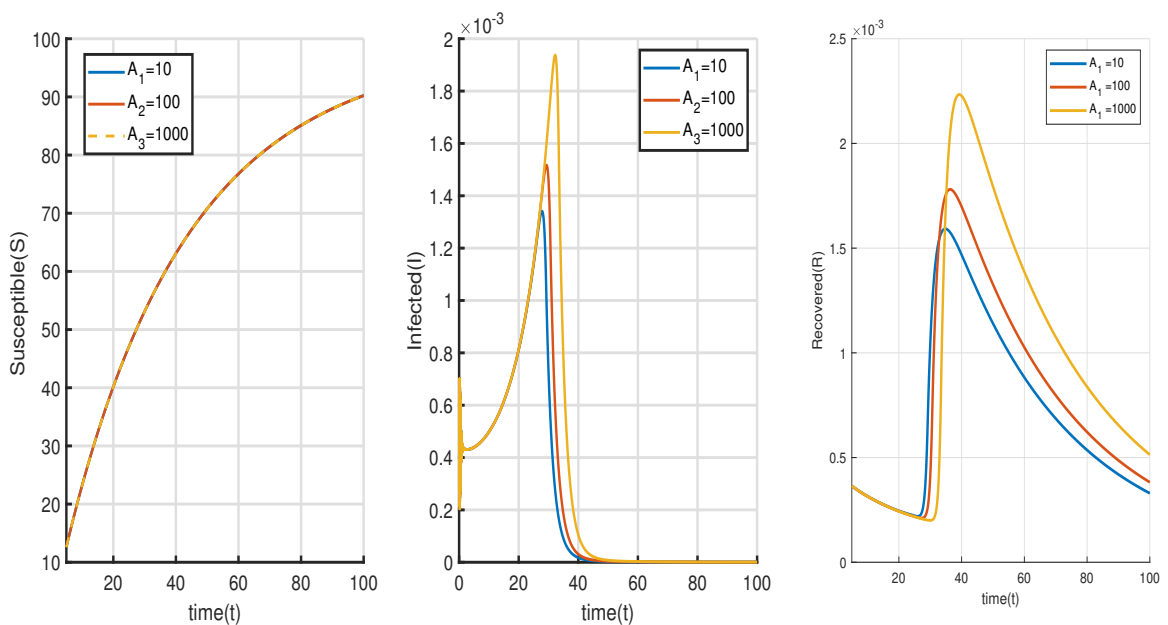
Figure 19. When $\alpha=0.9$, the time series of the model system (1) corresponds to Table 2
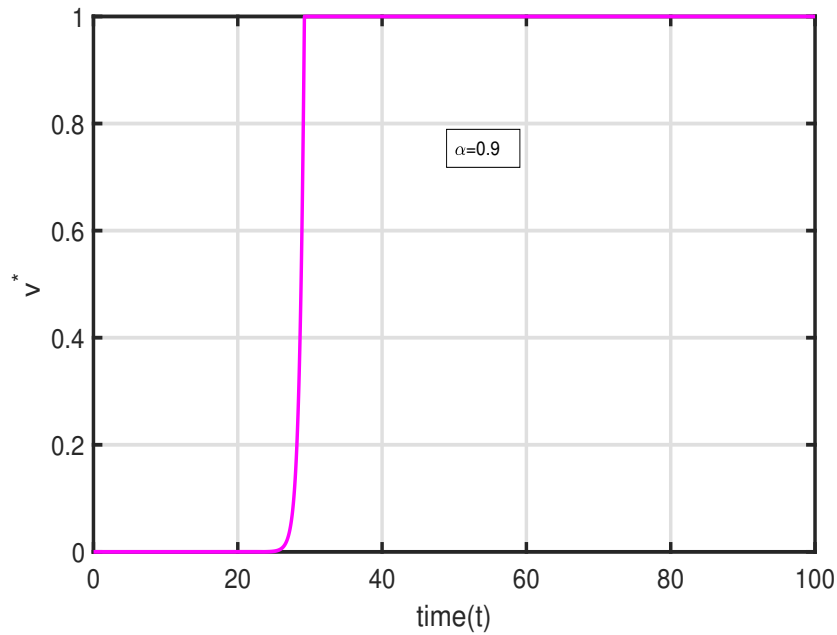
Figure 20. With parameter values matching to Table 2 for α=0.9, a time series of the ideal control variable v^* is produced

Figure 21. With parameter values matching to Table 2 for α=0.9, a time series of the ideal cost J^* is produced

8 Conclusion

The mathematical model used in this article aims to depict the dynamics of infectious disease when the ratio of infected to susceptible populations is high, taking into account the effects of inhibitory activity, behavioral changes that occur during epidemics, and the limitations of treatment facilities. Analyzing the stability characteristics of equilibrium points corresponding to no infection and

sustained infection states, it is shown that the disease-free equilibrium is locally asymptotically stable when $R_0 < 1$ and unstable when $R_0 > 1$.

The R-H criteria has been used to examine the stability of the model's endemic equilibrium. The simulation results predict that the infection will worsen as the rate of transmission rises, but that it will stabilize due to the accessibility of treatment centres. Furthermore, the prevalence of the infection decreases proportionally when the amount of suppression used by the affected people increases. The results of our simulation also showed that, in order to successfully eradicate the virus, the treatment of the population must be closely coordinated with the resources at hand. Understanding the complexities of disease outbreaks is made possible by the use of epidemic modelling. Numerical simulations provide the visualization of the efficacy of theoretical solutions. Comprehensive information, suitable infectious disease treatment methods, and the availability of healthcare services are required for the successful decrease of infection within society. In addition, we showed the global stability of the equilibrium state by choosing an appropriate Lyapunov function.

The importance of fractional order to population dynamics has also been noted. The optimum solution to the optimal control issue must meet certain requirements, which we have established using Pontryagin's Maximum Principle. It is obvious that the disease's spread can be stopped and eliminated if the control measure v^* is used. Additionally, Theorem 8 has identified the ideal control value v^* to reduce the cost of vaccination, as shown by $J(v) = \left(\int_0^{t_f} [I + A_1 v^2] \, dt \right)$. For optimum control, we presume a final time $t_f = 100$. As a consequence, changing the derivatives' order may change the stability requirements for equilibrium locations without changing any other parametric variables. We are unable to analyze our findings using an integer order method since we have achieved so little theoretical advancement in this fractional order framework. We find a variety of biological modelling outcomes based on fractional differential equations in this work. The proposed model may be analyzed further to explore chaotic solutions and various forms of bifurcations by incorporating time delay parameters. More than one control parameter may be used to better understand the treatment strategies and management of the spread of the disease.

Declarations

Use of AI tools

The authors declare that they have not used Artificial Intelligence (AI) tools in the creation of this article.

Data availability statement

All data generated or analyzed during this study are included in this article.

Ethical approval

The authors state that this research complies with ethical standards. This research does not involve either human participants or animals.

Consent for publication

Not applicable

Conflicts of interest

The authors declare that they have no conflict of interest.

Author's contributions

Conceptualization, Methodology, Software, Validation, Formal Analysis, Investigation, Resources, Data Curation, Writing - Original Draft, Writing - Review & Editing, Visualization, Supervision, Project Administration, Funding Acquisition. S.P.: Conceptualization, Writing - Review & Editing, Software, A.M.: Data Curation, Writing - Original Draft, Visualization, S.M.: Formal Analysis, Investigation, M.D.: Methodology, Supervision, Project Administration, P.C.M.: Methodology, Software, B.R.: Visualization, Supervision, Investigation, P.M.: Resources, Data Curation, Writing - Original Draft, P.B.: Investigation, Supervision, Project Administration. The authors have read and agreed to the published version of the manuscript.

References

[1] Kermack, W.O. and McKendrick, A.G. A contribution to the mathematical theory of epidemics. *Proceedings of the Royal Society of London. Series A,* 115(772), 700–721, (1927). [CrossRef]

[2] Kermack, W.O. and McKendrick, A.G. Contributions to the mathematical theory of epidemics-II: the problem of endemicity. *Proceedings of the Royal Society of London. Series A,* 138(834), 55–83, (1932). [CrossRef]

[3] Mukherjee, D. Stability analysis of an SI epidemic model with time delay. *Mathematical and Computer Modelling,* 24(9), 63–68, (1996). [CrossRef]

[4] Hethcote, H.W. and van den Driessche, P. An SIS epidemic model with variable population size and a delay. *Journal of Mathematical Biology,* 34, 177–194, (1995). [CrossRef]

[5] D'Onofrio, A., Manfredi, P. and Salinelli, E. Vaccinating behaviour, information, and the dynamics of SIR vaccine preventable diseases. *Theoretical Population Biology,* 71(3), 301–317, (2007). [CrossRef]

[6] Buonomo, B., d'Onofrio, A. and Lacitignola, D. Global stability of an SIR epidemic model with information dependent vaccination. *Mathematical Biosciences,* 216(1), 9–16, (2008). [CrossRef]

[7] Hattaf, K., Lashari, A., Louartassi, Y. and Yousfi, N. A delayed SIR epidemic model with a general incidence rate. *Electronic Journal of Qualitative Theory of Differential Equations,* 2023(3), 1–9, (2013). [CrossRef]

[8] Goel, K. and Nilam. Stability behavior of a nonlinear mathematical epidemic transmission model with time delay. *Nonlinear Dynamics,* 98, 1501–1518, (2019). [CrossRef]

[9] Kumar, A., Goel, K. and Nilam. A deterministic time-delayed SIR epidemic model: mathematical modeling and analysis. *Theory in Biosciences,* 139, 67–76, (2020). [CrossRef]

[10] Kumar, A. and Nilam. Dynamic behavior of an SIR epidemic model along with time delay; Crowley–Martin type incidence rate and holling type II treatment rate. *International Journal of Nonlinear Sciences and Numerical Simulation,* 20(7–8), 757–771, (2019). [CrossRef]

[11] Paul, S., Mahata, A., Mukherjee, S., Roy, B., Salimi, M. and Ahmadian, A. Study of fractional order SEIR epidemic model and effect of vaccination on the spread of COVID-19. *International*

Journal of Applied and Computational Mathematics, 8, 237, (2022). [CrossRef]

[12] Dubey, B., Patra, A., Srivastava, P.K. and Dubey, U.S. Modeling and analysis of an SEIR model with different types of nonlinear treatment rates. *Journal of Biological Systems,* 21(03), 1350023, (2013). [CrossRef]

[13] Paul, S., Mahata, A., Ghosh, U. and Roy, B. SEIR epidemic model and scenario analysis of COVID-19 pandemic. *Ecological Genetics and Genomics,* 19, 100087, (2021). [CrossRef]

[14] Tipsri, S. and Chinviriyasit, W. Stability analysis of SEIR model with saturated incidence and time delay. *International Journal of Applied Physics and Mathematics,* 4(1), 42–45, (2014). [CrossRef]

[15] Paul, S., Mahata, A., Mukherjee, S. and Roy, B. Dynamics of SIQR epidemic model with fractional order derivative. *Partial Differential Equations in Applied Mathematics,* 5, 100216, (2022). [CrossRef]

[16] Mahata, A., Paul, S., Mukherjee, S., Das, M. and Roy, B. Dynamics of Caputo fractional order SEIRV epidemic model with optimal control and stability analysis. *International Journal of Applied and Computational Mathematics,* 8, 28, (2022). [CrossRef]

[17] Mahata, A., Paul, S., Mukherjee, S. and Roy, B. Stability analysis and Hopf bifurcation in fractional order SEIRV epidemic model with a time delay in infected individuals. *Partial Differential Equations in Applied Mathematics,* 5, 100282, (2022). [CrossRef]

[18] Henderson, D.A. *Smallpox-The Death of a Disease.* Prometheus Books: Amherst, New York, USA, (2009).

[19] Samui, P., Mondal, J., Ahmad, B. and Chatterjee, A.N. Clinical effects of 2-DG drug restraining SARS-CoV-2 infection: a fractional order optimal control study. *Journal of Biological Physics,* 48, 415-438, (2022). [CrossRef]

[20] Shekhawat, U. and Roy Chowdhury (Chakravarty), A. Computational and comparative investigation of hydrophobic profile of spike protein of SARS-CoV-2 and SARS-CoV. *Journal of Biological Physics,* 48, 399-414, (2022). [CrossRef]

[21] Allegretti, S., Bulai, I.M., Marino, R., Menandro, M.A. and Parisi, K. Vaccination effect conjoint to fraction of avoided contacts for a Sars-Cov-2 mathematical model. *Mathematical Modelling and Numerical Simulation with Applications,* 1(2), 56-66, (2021). [CrossRef]

[22] Nindjin, A.F. and Aziz-Alaoui, M.A. Persistence and global stability in a delayed Leslie-Gower type three species food chain. *Journal of Mathematical Analysis and Applications,* 340(1), 340–357, (2008). [CrossRef]

[23] Iwa, L.L., Nwajeri, U.K., Atede, A.O., Panle, A.B. and Egeonu, K.U. Malaria and cholera co-dynamic model analysis furnished with fractional-order differential equations. *Mathematical Modelling and Numerical Simulation with Applications,* 3(1), 33-57, (2023). [CrossRef]

[24] Barman, D., Roy, J. and Alam, S. Trade-off between fear level induced by predator and infection rate among prey species. *Journal of Applied Mathematics and Computing,* 64, 635–663, (2020). [CrossRef]

[25] Das, P., Nadim, S.S., Das, S. and Das, P. Dynamics of COVID-19 transmission with comorbidity: a data driven modelling based approach. *Nonlinear Dynamics,* 106, 1197–1211, (2021). [CrossRef]

[26] Das, S., Das, P. and Das, P. Optimal control of behaviour and treatment in a nonautonomous SIR model. *International Journal of Dynamical Systems and Differential Equations,* 11(2), 108-130, (2021). [CrossRef]

[27] Das, P., Upadhyay, R.K., Misra, A.K., Rihan, F.A., Das, P. and Ghosh, D. Mathematical model of COVID-19 with comorbidity and controlling using non-pharmaceutical interventions and vaccination. *Nonlinear Dynamics,* 106, 1213-1227, (2021). [CrossRef]

[28] Capasso, V. and Serio, G. A generalization of the Kermack-Mckendrick deterministic epidemic model. *Mathematical Biosciences,* 42(1–2), 43–61, (1978). [CrossRef]

[29] D'Onofrioa, A. and Manfredi, P. Information-related changes in contact patterns may trigger oscillations in the endemic prevalence of infectious diseases. *Journal of Theoretical Biology,* 256(3), 473–478, (2009). [CrossRef]

[30] Wei, C. and Chen, L. A delayed epidemic model with pulse vaccination. *Discrete Dynamics in Nature and Society,* 2008, 746951, (2008). [CrossRef]

[31] Capasso, V., Grosso, E. and Serio, G. Mathematical models in epidemiological studies. I. Application to the epidemic of cholera verified in Bari in 1973. *Annali Sclavo; Rivista di Microbiologia e di Immunologia,* 19(2), 193–208, (1977).

[32] Capasso, V. Global solution for a diffusive nonlinear deterministic epidemic model. *SIAM Journal on Applied Mathematics,* 35(2), 274–284, (1978). [CrossRef]

[33] Zhang, J.Z., Jin, Z., Liu, Q.X. and Zhang, Z.Y. Analysis of a delayed SIR model with nonlinear incidence rate. *Discrete Dynamics in Nature and Society,* 2008, 636153, (2008). [CrossRef]

[34] Anderson, R.M. and May, R.M. Regulation and stability of host-parasite population interactions: I. Regulatory processes. In *Foundations of Ecology II,* (pp. 219–267). USA: University of Chicago Press, (1978). [CrossRef]

[35] Li, X.Z., Li, W.S. and Ghosh, M. Stability and bifurcation of an SIR epidemic model with nonlinear incidence and treatment. *Applied Mathematics and Computation,* 210(1), 141-150, (2009). [CrossRef]

[36] Hammouch, Z., Yavuz, M. and Özdemir, N. Numerical solutions and synchronization of a variable-order fractional chaotic system. *Mathematical Modelling and Numerical Simulation with Applications,* 1(1), 11-23, (2021). [CrossRef]

[37] Daşbaşı, B. Stability analysis of an incommensurate fractional-order SIR model. *Mathematical Modelling and Numerical Simulation with Applications,* 1(1), 44-55, (2021). [CrossRef]

[38] Gholami, M., Ghaziani, R.K. and Eskandari, Z. Three-dimensional fractional system with the stability condition and chaos control. *Mathematical Modelling and Numerical Simulation with Applications,* 2(1), 41-47, (2022). [CrossRef]

[39] Wang, W. and Ruan, S. Bifurcations in an epidemic model with constant removal rate of the infectives. *Journal of Mathematical Analysis and Applications,* 291(2), 775-793, (2004). [CrossRef]

[40] Zhang, X. and Liu, X. Backward bifurcation of an epidemic model with saturated treatment function. *Journal of Mathematical Analysis and Applications,* 348(1), 433-443, (2008). [CrossRef]

[41] Zhonghua, Z. and Yaohong, S. Qualitative analysis of a SIR epidemic model with saturated treatment rate. *Journal of Applied Mathematics and Computing,* 34, 177–194, (2010). [CrossRef]

[42] Zhou, L. and Fan, M. Dynamics of an SIR epidemic model with limited medical resources revisited. *Nonlinear Analysis: Real World Applications,* 13(1), 312-324, (2012). [CrossRef]

[43] Dubey, B., Patra, A., Srivastava, P.K. and Dubey, U.S. Modeling and analysis of an SEIR model with different types of nonlinear treatment rates. *Journal of Biological Systems,* 21(03), 1350023, (2013). [CrossRef]

[44] Kumar, A. and Nilam. Dynamical model of epidemic along with time delay; Holling type II

incidence rate and Monod-Haldane type treatment rate. *Differential Equations and Dynamical Systems,* 27, 299–312, (2019). [CrossRef]

[45] Diethelm, K. and Ford, N.J. Analysis of fractional differential equations. *Journal of Mathematical Analysis and Applications,* 265(2), 229-248, (2002). [CrossRef]

[46] Rahaman, M., Mondal, S.P., Alam, S., Metwally, A.S.M., Salahshour, S., Salimi, M. et al. Manifestation of interval uncertainties for fractional differential equations under conformable derivative. *Chaos Solitons & Fractals,* 165, 112751, (2022). [CrossRef]

[47] Barman, D., Roy, J., Alrabaiah, H., Panja, P., Mondal, S.P. and Alam, S. Impact of predator incited fear and prey refuge in a fractional order prey predator model. *Chaos Solitons & Fractals,* 142, 110420, (2021). [CrossRef]

[48] Nguyen, T.T.H., Nguyen, N.T. and Tran, M.N. Global fractional Halanay inequalities approach to finite-time stability of nonlinear fractional order delay systems. *Journal of Mathematical Analysis and Applications,* 525(1), 127145, (2023). [CrossRef]

[49] Petras, I. *Fractional-Order Nonlinear Systems: Modeling, Analysis and Simulation.* Higher Education Press: Beijing, China, (2011).

[50] Odibat, Z.M. and Shawagfeh, N.T. Generalized Taylor's formula. *Applied Mathematics and Computation,* 186(1), 286-293, (2007). [CrossRef]

[51] Podlubny, I. *Fractional Differential Equations.* Academic Press: San Diego, (1999).

[52] Liang, S., Wu, R. and Chen, L. Laplace transform of fractional order differential equations. *Electronic Journal of Differential Equations,* 2015(139), 1-15, (2015).

[53] Mainardi, F. On some properties of the Mittag-Leffler function $E_\alpha(-t^\alpha)$, completely monotone for $t > 0$ with $0 < \alpha < 1$. *Discrete and Continuous Dynamical Systems Series B,* 19(7), 2267-2278, (2014). [CrossRef]

[54] Li, Y., Chen, Y. and Podlubny, I. Stability of fractional-order nonlinear dynamic systems: Lyapunov direct method and generalized Mittag-Leffler stability. *Computers & Mathematics with Applications,* 59(5), 1810-1821, (2010). [CrossRef]

[55] Javidi, M. and Nyamoradi, N. A fractional-order toxin producing phytoplankton and zooplankton system. *International Journal of Biomathematics,* 7(04), 1450039, (2014). [CrossRef]

[56] Diekmann, O., Heesterbeek, J.A.P. and Roberts, M.G. The construction of next-generation matrices for compartmental epidemic models. *Journal of the Royal Society Interface,* 7(47), 873-885, (2009). [CrossRef]

[57] Kumar, A. and Nilam. Effects of nonmonotonic functional responses on a disease transmission model: modeling and simulation. *Communications in Mathematics and Statistics,* 10, 195–214, (2022). [CrossRef]

[58] Ding, Y., Wang, Z. and Ye, H. Optimal control of a fractional-order HIV-immune system with memory. *IEEE Transactions on Control Systems Technology,* 20(3), 763-769, (2011). [CrossRef]

[59] Agarwal, O.P. A general formulation and solution scheme for fractional optimal control problems. *Nonlinear Dynamics,* 38, 323-337, (2004). [CrossRef]

[60] Kamocki, R. Pontryagin maximum principle for fractional ordinary optimal control problems. *Mathematical Methods in the Applied Sciences,* 37(11), 1668-1686, (2014). [CrossRef]

(https://bulletinbiomath.org)